Earth Planets Space, **53**, 949–958, 2001

On the calibration of a vectorial ^{4}He pumped magnetometer

O. Gravrand[1], A. Khokhlov[2,3], J. L. Le Mouël[3], and J. M. Léger[1]

[1]*Laboratoire d'Electronique et de Technique d'Instrumentation, Commissariat à l'énergie atomique, referred to later on as CEA/LETI Grenoble - 17 rue des martyrs - 38054 Grenoble cedex 9, France*
[2]*International Institute of Earthquake Prediction Theory and Mathematical Geophysics 79, b2, Warshavskoe shosse 113556 Moscow, Russia*
[3]*Institut de Physique du Globe de Paris, 4, Place Jussieu, 75252, Paris, France*

(Received October 30, 2000; Revised April 17, 2001; Accepted May 28, 2001)

The prototype of a ^{4}He pumped vector magnetometer is presented. Large auxiliary coils systems used in previously developed apparatus to allow vector measurements from a scalar (atomic or nuclear resonance) sensor are replaced by a light triaxial modulation system associated with advanced techniques of signal processing. The performances of the helium scalar sensor are first briefly recalled; then the principle of the vector measurement, obtained by adding three (approximately) orthogonal modulations of different frequencies (all of the order of 10 Hz) is explained. Afterwards a second part of the paper is devoted to the calibration process, and a first estimate of the performances of the vector magnetometer is obtained. They confirm that this instrument could be a good candidate for an automatic absolute magnetic observatory: after the calibration process completion and a proper installation, it would provide by itself the absolute value of three orthogonal components of the field. In addition to that, the ^{4}He vector magnetometer appears to be also promising for space applications.

1. Introduction

The idea of designing a vector magnetometer based on an atomic or nuclear resonance sensor—delivering by itself only measurements of intensity of the magnetic field—by adding auxiliary equipment is not new. A pioneering realization was the automatic standard magnetic observatory (ASMO) of L. R. Alldredge (1960–1964) (Alldredge, 1960; Alldredge and Saldukas, 1964) built around a rubidium vapor self oscillating magnetometer. The auxiliary equipment consisted of two mutually perpendicular pairs of coils which controlled bias fields in a plane perpendicular to the mean magnetic field vector. Such an instrument was installed at Fredericksburg observatory.

Following it, several "absolute" vector magnetometers were built from a proton or atomic resonance sensor and a system of coils. Some of them were commercialized (such as the ELSEC), many were constructed by scientists working in scientific institutions and magnetic observatories (as the big coils system of Kasmmer in Kakioka observatory). In fact, most of these magnetometers were used only for sporadic absolute measurements the way the classical inductometers and theodolites (with the Gauss-Lamont method to measure the horizontal component) used to be. Their performances, according to our experience, were reasonably good (except for the measurement of the component perpendicular to the geographic meridian). The introduction in the early 80's of D.I. flux (D for declination, I for inclination, flux for fluxgate) theodolite, very easy to handle, coupled with a proton or atomic resonance scalar sensor, reduced the interest for such systems.

In any case, the objective of an automatic observatory combining—according to the views of Alldredge—"the measurement of magnetic variations and absolute values", has been abandoned almost everywhere. The main reason is that, without an independent absolute control, the systems made of a scalar sensor and a coils system are subject to important drifts. And, as soon as regular independent absolute measurements are required, it is much more practical to use fluxgate (for example) variometers.

Nevertheless, the project of an automatic (standard) magnetic observatory has conserved all its interest. The number of magnetic observatories operated at the Earth's surface is dramatically insufficient, with furthermore a very poor geographical distribution (which raises the question of sea bottom observatories). The availability of an automatic observatory would greatly help to improve the situation. Let us recall the performances that such an equipment should reach (adopting Intermagnet, Trigg and Coles (1999) claimed standards for classical observatories): provide the absolute values of three components of the magnetic field with an accuracy of the order of 1 nT, without independent absolute control (or more probably with a control by independent long spaced absolute measurements, for example once a year; no strict rule is to be given there).

The present helium pumped vector magnetometer challenges such an objective. Its main originality is that it replaces complicated mechanical devices such as large coils systems with drift prone axes by a light triaxial modulation system associated with advanced techniques of signal processing. Furthermore, whereas ASMO was a pulsed magnetometer, the helium magnetometer is a continuous instru-

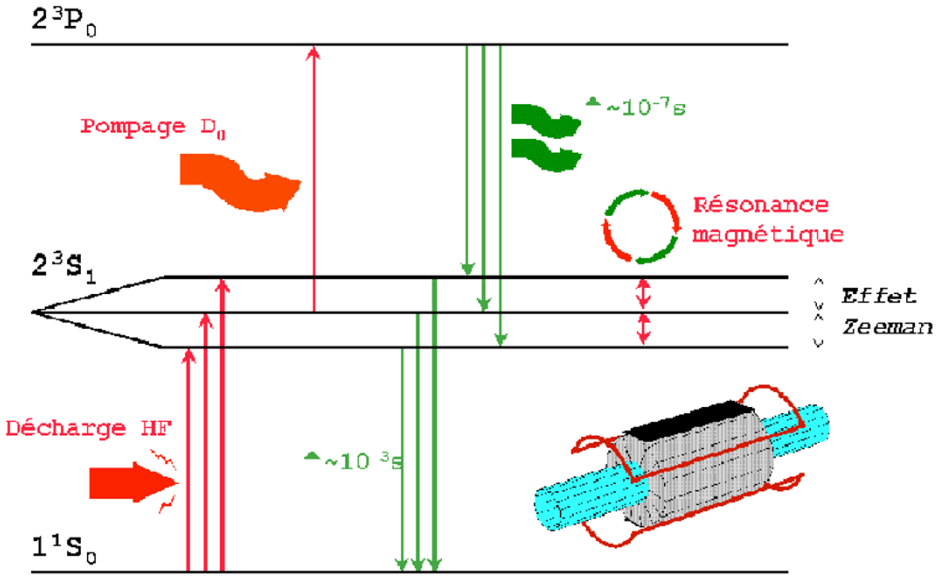

Fig. 1. ^{4}He energy diagram.

ment, which allows a perfect control of the noise spectrum and prevents from aliasing problems.

Efforts to conceive and realize automatic magnetic observatories (with the objective of requesting only long spaced absolute measurements) are unfortunately rather few. Let us quote the system presently developed at the Institut Royal météorologique in Belgium (Rasson, 1994) which consists of an automated DI flux theodolite intended indeed for making unattended measurements of the declination and inclination in an observatory environment. Rasson's magnetometer is also planned for sea-bottom observations. Let us quote also the $\Delta I \Delta D$ system (delta I delta D) presently developed in Hungary, France and US, although its objective is more to allow interpolations between classical absolute measurements than to construct a genuine automatic observatory.

2. Principle of the Helium Vector Magnetometer

The magnetometer which will be described in this paper, together with its calibration technique—which we will focus on—intends to provide an absolute measurement of the intensity of the magnetic field together with its components along three stable axes simultaneously and at the same place. This type of sensor delivers redundant information in the sense that the calculated modulus obtained thanks to the vector measurements can be compared with the direct intensity (scalar) measurement. The idea of this paper is to use this redundancy to estimate the calibration parameters needed for the vector measurement. This method has been applied for a long time to calibrate space magnetometers (Merayo *et al.*, 2000); it will be used here in an original way.

2.1 The scalar helium pumped magnetometer. Principles of operation and description

Over the past few years, CEA/LETI has been involved in the development of an isotropic ^{4}He pumped magnetometer (Guttin *et al.*, 1993).

Helium magnetometers are based on an electronic magnetic resonance whose effects are amplified by a laser pumping process. The first step is to excite a fraction of the helium atoms to the 2^3S_1 metastable state by means of a high frequency discharge. This energy level it split by the static magnetic field H_o into three Zeeman sublevels (Colegrove and Schearer, 1961). The measurement of their energy separation provides then a very convenient means to determine the earth field.

This is performed thanks to a magnetic resonance experiment. Hence, the second step is to induce transitions between the sublevels in order to detect the resonance. If the applied radiofrequency field matches the Larmor frequency of the Zeeman sublevels, transitions between these sublevels occur and tend to equalize their populations. However, the resonance signal amplitude is very low since at thermal equilibrium the sublevels are almost equally populated and no significant change subsequently results from the resonance. So the third step is to modify the repartition of the atoms within the three sublevels (alignment or polarization of the metastable state). This is accomplished by optically pumping helium atoms with a tuned laser: atoms in the 2^3S_1 metastable state absorb the laser light with different probabilities for each sublevel and are thus selectively excited to the 2^3P_0 state (Fig. 1). From there, they undergo a spontaneous emission back to the metastable state. Thanks to this process, the resonance signal amplitude is enhanced by several orders of magnitude.

The resonance can be detected by monitoring the transmitted laser intensity: when the resonance condition is met, the polarization of the metastable state created as a result of the optical pumping process is reduced by the RF field so that the helium cell transparency decreases. The RF field frequency is then phase locked by an electronic loop to the Larmor frequency, resulting in a field/frequency transducer which can be used as a high sensitivity magnetometer.

Principles of the scalar helium magnetometer are illus-

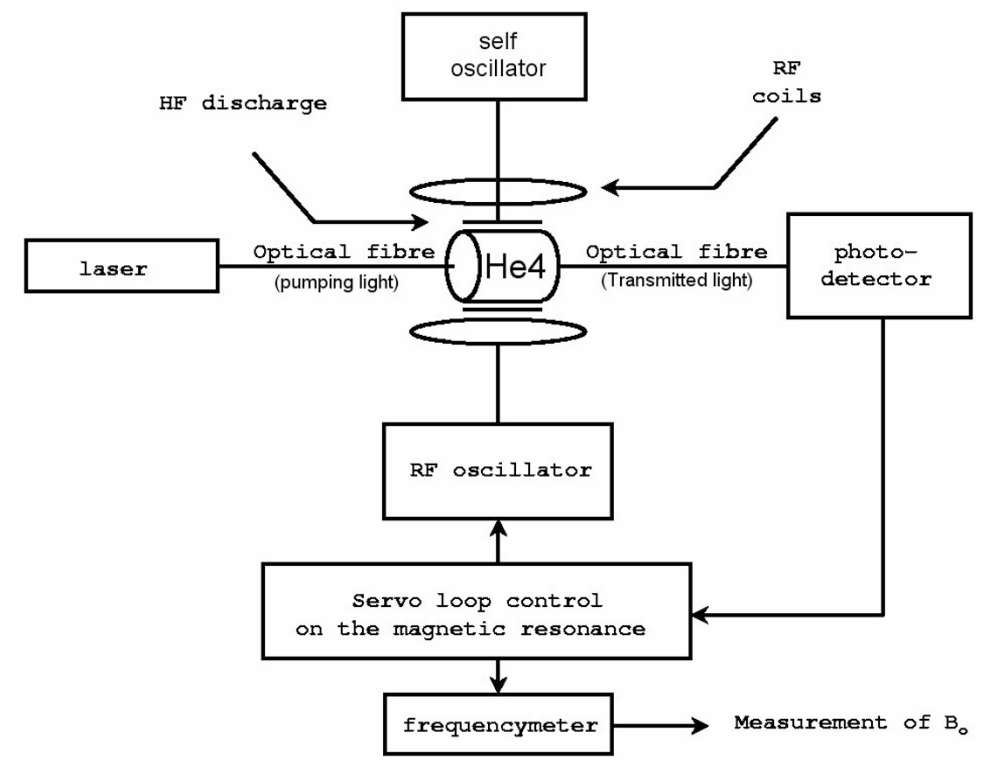

Fig. 2. Architecture of the scalar ^{4}He pumped magnetometer.

trated by Fig. 2. The apparatus has the following performances.

a) Very high sensitivity: of the order of 1 pT/$\sqrt{\text{Hz}}$. The r.m.s noise results from the integration of the noise density over the sensor bandwith (see below): B (nTrms) $= \sqrt{\Delta B} \times B$ (nT/$\sqrt{\text{Hz}}$); taking $\Delta B =$ 1 Hz, a 1 pT/$\sqrt{\text{Hz}}$ noise density is equivalent to a 1 pT noise level.

b) Bandwidth: DC to 200–300 Hz.

c) Absolute accuracy: better than 100 pT. The absolute accuracy takes into account various phenomena such as thermal drift, uncertainties on the exact value of the metastable helium gyromagnetic ratio, measurement offsets induced by the sensor head materials. For comparison, the NMR scalar magnetometers which have been developed by LETI for the Ørsted and Champ satellite missions were specified for an absolute accuracy of ±250 pT.

d) Range of measured field: [5 μT, 100 μT] with no signal to noise ratio variation.

2.2 Principle of the vector measurement

Thanks to the combination of characteristics a and b, it is possible to design a continuous vector magnetometer by adding three orthogonal modulations β^1, β^2, β^3 (1,2,3 refer to the axes of the triaxial coil system $\{\vec{\mathbf{e}}_1, \vec{\mathbf{e}}_2, \vec{\mathbf{e}}_3\}$ used to generate these modulations) to the geomagnetic field $\vec{\mathbf{B}}$ seen by the sensing cell. Characteristics a and b are indeed necessary to design a continuous vector magnetometer based on a scalar sensor. It is indeed requested to

i) use permanent modulations to avoid aliasing,

ii) make sure that the magnetometer adequately follows the magnetic field variations resulting from these modulations; this constraint implies a high bandwith of the scalar sensor,

iii) use a very sensitive scalar magnetometer to obtain good vector measurements since these latter measurements are much less sensitive than the scalar ones (see explanation below formula (2)).

The scalar magnetometer measures the modulus of the resulting field:

$$|\vec{\mathbf{B}}_{\text{tot}}| = \left| \vec{\mathbf{B}} + \sum_{j=1}^{3} \beta^j \cos(\omega_j t) \vec{\mathbf{e}}_j \right| \tag{1}$$

where ω_j are the modulation pulsations.

The vector measurement is obtained by processing the 32 bits numerical output of the scalar measurement (1). This scalar output contains several spectral components as can be seen on Fig. 3:

- a DC component
- principal harmonics at ω_j pulsations
- second order harmonics at pulsations $2\omega_j$ and $\omega_j \pm \omega_{j'}$.

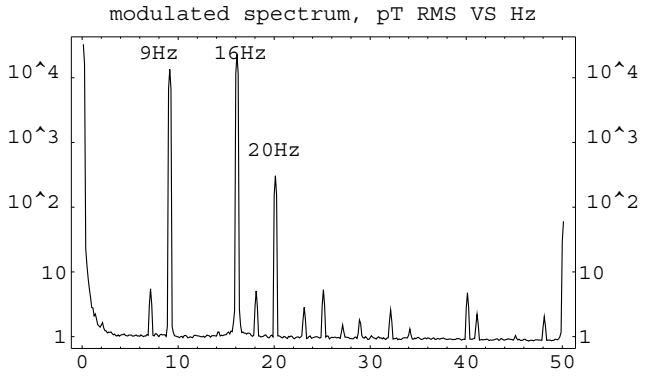

Fig. 3. Spectral density of the signal obtained with the modulated scalar ^{4}He pumped magnetometer when the sensor is submitted to the three modulations (modulations ω_j at 9 Hz, 16 Hz and 20 Hz).

In the hypothesis of a slowly varying magnetic field $\vec{\mathbf{B}}$ (varying with time constants small with respect to the modulation frequencies), and modulation amplitudes of the order of $10^{-3}|\vec{\mathbf{B}}|$, the DC component can be interpreted as a measurement of the magnetic field modulus $b = |\vec{\mathbf{B}}|$ (but see Subsection 2.3), and principal harmonics h^1, h^2 and h^3 (which denote the measured amplitudes) are proportional to the projections of the vector $\vec{\mathbf{B}}$ onto the 3 axes of modulation:

$$h^j = \frac{\beta^j(\vec{\mathbf{B}} \cdot \vec{\mathbf{e}}_j)}{b} \tag{2}$$

A first objective of the vector magnetometer is to retrieve $\vec{\mathbf{B}} \cdot \vec{\mathbf{e}}_j$, $(j = 1, 2, 3)$ from the scalar data b, h^j. From the above formula (2), this is possible once the β^j are known. Attention has to be paid to the fact that the projection $\vec{\mathbf{B}} \cdot \vec{\mathbf{e}}_j$ will be deduced through a very high noise amplification factor $b/\beta \cong 10^3$: a noise of 1 pT/$\sqrt{\text{Hz}}$ on h^j will be interpreted as a noise of 1 nT/$\sqrt{\text{Hz}}$ on the projection. Therefore, very high precision and sensitivity are needed in the measurements of the h^j's. Moreover, if β^j fluctuates of say 10 ppm, this will be interpreted by the vector instrument as a 10 ppm fluctuation of $\mathcal{B}^j = \vec{\mathbf{B}} \cdot \vec{\mathbf{e}}_j$. Modulation amplitudes must therefore be well known and controlled in order to make accurate measurements. To avoid fluctuations, special care has been taken to realize the modulation coils set and the modulation current generator:

- High purity silica has been used for the coils supports, resulting in a mechanical stability of 5×10^{-7} K^{-1}
- A highly stable electronics has been designed (with a temperature dependence smaller than 10^{-6} K^{-1})

In any case, the direct knowledge of the coils transfer functions and of the electrical current source characteristics does not provide the β^j with a sufficient accuracy: a calibration is necessary.

Projections $\vec{\mathbf{B}} \cdot \vec{\mathbf{e}}_j$ on the sensor frame axes $\{\vec{\mathbf{e}}_1, \vec{\mathbf{e}}_2, \vec{\mathbf{e}}_3\}$ will be then available. But again the $\vec{\mathbf{e}}_j$ are only approximately known. In order to take benefit of the 1 nT/$\sqrt{\text{Hz}}$ noise on the vector measurement (see above), a precision of $10^{-5} rad$ is required on the modulation directions $\vec{\mathbf{e}}_j$ determination, which cannot be guaranteed by construction. A calibration process is once more necessary to determine the $\vec{\mathbf{e}}_j$ with the required precision. In fact, concerning the directional calibration in the present paper, we will limit ourselves to the accurate determination of the angles between the axes of the sensor frame (see Section 4).

It might be said that we are faced with the need of a "strain" calibration (the β^j) and a directional calibration (the $\vec{\mathbf{e}}_j$). Before presenting in detail the calibration process, let us note that the vector measurement delivered by such a sensor is free of offsets, which is an important advantage over fluxgate directional magnetometers (Nielsen *et al.*, 1995), for which in fact three additional parameters must also be estimated during the calibration process.

2.3 Consequence of the modulations on the scalar absolute measurement

The DC component of the output is taken as the measurement of the modulus $b = |\vec{\mathbf{B}}|$. Note nevertheless that any modulation not aligned with the static magnetic field $\vec{\mathbf{B}}$ induces an aliasing of the second order harmonics (whose amplitudes are noted h^{2j}, $2j$ standing for the double of the modulation frequency on the j axis) onto the continuous level DC; therefore, in fact:

$$\text{DC} = b - \sum_{j=1,2,3} h^{2j} \tag{3}$$

with:

$$h^{2j} = \frac{(\beta^j)^2}{4b}\left[1 - \left(\frac{\vec{\mathbf{B}} \cdot \vec{\mathbf{e}}_j}{b}\right)^2\right]$$

In the case of a perfect triorthogonal coils set and identical modulation amplitudes ($\beta^1 = \beta^2 = \beta^3 = \beta$) along the three axes, the aliasing term remains independent of the direction of the field. Moreover, its magnitude is very low in a 50 μT magnetic field:

$$\sum_{j=1,2,3} h^{2j} = \frac{(\beta)^2}{4b}\left[3 - \sum_{j=1,2,3}\left(\frac{\vec{\mathbf{B}} \cdot \vec{\mathbf{e}}_j}{b}\right)^2\right]$$
$$= \frac{1}{2}\frac{(\beta)^2}{b} \cong 25 \text{ pT}.$$

In practice, skewness in the axes and differences between the β^j's may occur and thus may cause the aliasing to vary with the direction of $\vec{\mathbf{B}}$. However, the average value of this error is very small (25 pT) and its variations will be smaller by several orders of magnitude, and therefore negligible (remember that the values of β^j have to be stable up to 1 ppm·K^{-1}). Actually this aliasing is safely neglected in the calibration algorithm. But one must keep its existence in mind as it induces a systematic error (which can however be easily systematically corrected if necessary), on the scalar absolute measurement.

3. Description of the Calibration Problem

3.1 Notations

Let us consider the magnetic field vector $\vec{\mathbf{B}}$ defined in the 3-dimensional real vector space $\mathbb{R}^3$ equipped with a *cartesian* frame with unit vectors $\{\vec{\mathbf{u}}_1, \vec{\mathbf{u}}_2, \vec{\mathbf{u}}_3\}$ (which would be

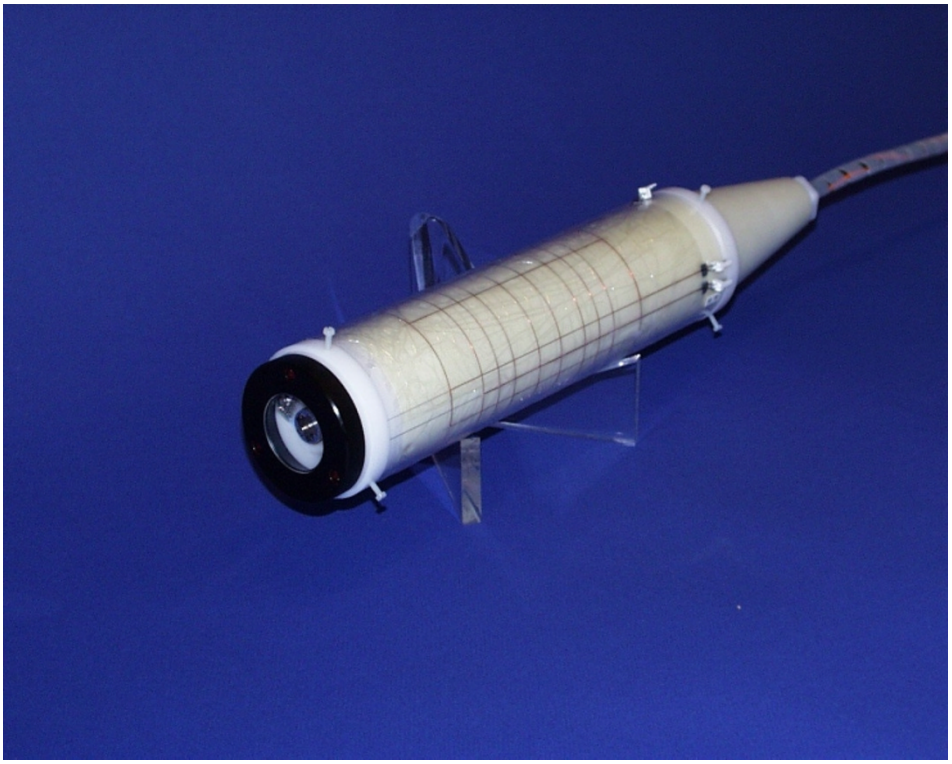

Fig. 4. Triaxial vector helium pumped sensor developed at LETI. (length 30 cm; diameter 6 cm)

for example the geophysical frame: horizontal North, horizontal East, downwards vertical).

We list the notations in use for measured and unknown quantities:

$b = |\vec{\mathbf{B}}|$ is the measurement of the magnetic field modulus (neglecting the second order aliasing);

$\vec{\mathbf{e}}_j$ is the unit vector of the corresponding modulation direction (unknown);

β^j denotes the modulation amplitude (unknown positive value) along the corresponding direction; $\Lambda = \Lambda^*$ is the matrix of modulation amplitudes ($*$ is for transposition):

$$\Lambda = \begin{matrix} \beta^1 & 0 & 0 \\ 0 & \beta^2 & 0 \\ 0 & 0 & \beta^3 \end{matrix} \tag{4}$$

$\mathcal{B}^j = \vec{\mathbf{B}} \cdot \vec{\mathbf{e}}_j$ is the projection of $\vec{\mathbf{B}}$ on the direction $\vec{\mathbf{e}}_j$; we denote $\vec{\mathfrak{B}}$ the triplet $(\mathcal{B}^1, \mathcal{B}^2, \mathcal{B}^3)$ of such projections (unknown).

We shall use the subscript index for the sequence of modulus measurements b_k, sequence of harmonics

$$h_k^j = \frac{\beta^j \mathcal{B}_k^j}{b_k} \tag{5}$$

and sequences of related quantities $\vec{\mathbf{B}}_k$, $\mathcal{B}_k^j$ etc. Thus we are given the basic data set $\left\{b_k, \vec{\mathbf{H}}_k\right\} = \left\{b_k, h_k^1, h_k^2, h_k^3\right\}$, $k = 1, \ldots N$. The matricial version of expression (5) is:

$$\vec{\mathfrak{B}}_k = b_k \cdot \vec{\mathbf{H}}_k \cdot \Lambda^{-1} \tag{6}$$

3.2 The problem

We aim first to recover from the data the unknown internal parameters of the magnetometer—the modulation amplitudes β^j and the corresponding directions $\vec{\mathbf{e}}_j$—. The second problem is to recover the available information about the vectors $\vec{\mathbf{B}}_k$, $k = 1, \ldots N$. Let us consider both these problems in more details.

The complete description of the vector $\vec{\mathbf{B}}_k$ (for a given k) consists in its decomposition in the given cartesian frame $\{\vec{\mathbf{u}}_1, \vec{\mathbf{u}}_2, \vec{\mathbf{u}}_3\}$ or (which is equivalent) its decomposition in any other frame for which the coordinates transformation to the $\{\vec{\mathbf{u}}_j\}$ is known. In fact, for a given data set $\left\{b_k, h_k^1, h_k^2, h_k^3\right\}$, even with known parameters β^1, β^2 and β^3, but without any other additional measurements, there is no chance for the unit vectors $\vec{\mathbf{e}}_1$, $\vec{\mathbf{e}}_2$ and $\vec{\mathbf{e}}_3$ to be absolutely recovered with respect to the cartesian frame $\{\vec{\mathbf{u}}_1, \vec{\mathbf{u}}_2, \vec{\mathbf{u}}_3\}$. This is because we can always rotate rigidly the system made of the three modulation directions and vector $\vec{\mathbf{B}}$. This means that we have to look at most for the angles $\widehat{\vec{\mathbf{e}}_k \vec{\mathbf{e}}_j}$ (or scalar products $\vec{\mathbf{e}}_k \cdot \vec{\mathbf{e}}_j = \cos(\widehat{\vec{\mathbf{e}}_k \vec{\mathbf{e}}_j})$) and for the corresponding linear decomposition of $\vec{\mathbf{B}}$ in this frame. In other words, we only consider the *internal calibration* problem.

3.3 Auxiliary formulas

3.3.1 The expression of components versus projections Let B^1, B^2, B^3 be the *components* of the linear decomposition $\vec{\mathbf{B}} = B^1\vec{\mathbf{e}}_1 + B^2\vec{\mathbf{e}}_2 + B^3\vec{\mathbf{e}}_3$ of the vector $\vec{\mathbf{B}}$ in the *non-orthogonal* sensor frame $\vec{\mathbf{e}}_j$. The three equations linking the components B_k^1, B_k^2 and B_k^3 and the projections $\mathcal{B}_k^1$,

$\mathcal{B}_k^2$ and $\mathcal{B}_k^3$ of the vector $\vec{\mathbf{B}}$ onto the *non-orthogonal* frame axes $\{\vec{\mathbf{e}}_1, \vec{\mathbf{e}}_2, \vec{\mathbf{e}}_3\}$ are

$$\begin{cases} \sum_{j=1}^{3} B_k^j (\vec{\mathbf{e}}_j \cdot \vec{\mathbf{e}}_1) = \mathcal{B}_k^1 \\ \sum_{j=1}^{3} B_k^j (\vec{\mathbf{e}}_j \cdot \vec{\mathbf{e}}_2) = \mathcal{B}_k^2 \\ \sum_{j=1}^{3} B_k^j (\vec{\mathbf{e}}_j \cdot \vec{\mathbf{e}}_3) = \mathcal{B}_k^3 \end{cases} \tag{7}$$

This may be expressed in a matrix form if we denote $\mathbf{A}$ the 3×3-matrix of the scalar products $\vec{\mathbf{e}}_k \cdot \vec{\mathbf{e}}_j = \cos(\widehat{\vec{\mathbf{e}}_k \vec{\mathbf{e}}_j})$:

$$\begin{aligned} \vec{\mathbf{B}}_k \cdot \mathbf{A} &= \vec{\mathfrak{B}}_k \\ \vec{\mathbf{B}}_k &= \vec{\mathfrak{B}}_k \cdot \mathbf{A}^{-1} \end{aligned} \tag{8}$$

where $\mathbf{A}^{-1}$ is for the inverse of matrix $\mathbf{A}$. So, to determine the components B_k^j in the non-cartesian frame it is enough to know the projections $\mathcal{B}_k^j$ onto the axes of this frame and matrix $\mathbf{A}$. Let $\mathbf{C}$ be the matrix mapping the frame $\{\vec{\mathbf{u}}_1, \vec{\mathbf{u}}_2, \vec{\mathbf{u}}_3\}$ onto the $\{\vec{\mathbf{e}}_1, \vec{\mathbf{e}}_2, \vec{\mathbf{e}}_3\}$ one:

$$\begin{matrix} \vec{\mathbf{e}}_1 \\ \vec{\mathbf{e}}_2 \\ \vec{\mathbf{e}}_3 \end{matrix} = \mathbf{C} \begin{matrix} \vec{\mathbf{u}}_1 \\ \vec{\mathbf{u}}_2 \\ \vec{\mathbf{u}}_3. \end{matrix} \tag{9}$$

From (7), (9), as $\{\vec{\mathbf{u}}_1, \vec{\mathbf{u}}_2, \vec{\mathbf{u}}_3\}$ is *orthonormal*, it comes

$$\mathbf{A} = \mathbf{C}\mathbf{C}^*$$

Note that $\mathbf{A}$ depends only on departures of $\{\vec{\mathbf{e}}_j\}$-frame from orthogonality; this means—as said earlier—that $\{\vec{\mathbf{e}}_j\}$-frame can be recovered only within a solid rotation.

3.3.2 The expressions of the modulus Let us express the relation between the modulus of vector $\vec{\mathbf{B}}_k$ and its projections (onto the axes of the non-cartesian frame). Using Eqs. (8) and

$$|\vec{\mathbf{B}}_k|^2 = \vec{\mathbf{B}}_k \cdot \mathbf{A} \cdot \vec{\mathbf{B}}_k^*$$

we get

$$|\vec{\mathbf{B}}_k|^2 = \vec{\mathfrak{B}}_k \cdot \mathbf{A}^{-1} \cdot \vec{\mathfrak{B}}_k^* \tag{10}$$

where $\vec{\mathbf{B}}^*$, $\vec{\mathfrak{B}}^*$ are for the transposed vectors.

3.4 The basic relation and the solution algorithm

From Eqs. (5) and (10) we get a system of linear equations for the entries of matrix $\mathbf{G}$:

$$\begin{cases} \vec{\mathbf{H}}_1 \mathbf{G} \vec{\mathbf{H}}_1^* = 1 \\ \vec{\mathbf{H}}_2 \mathbf{G} \vec{\mathbf{H}}_2^* = 1 \\ \cdots \\ \vec{\mathbf{H}}_N \mathbf{G} \vec{\mathbf{H}}_N^* = 1 \end{cases} \tag{11}$$

with

$$\mathbf{G}^{-1} = \Lambda \mathbf{A} \Lambda^*.$$

We may assume this system to be overdetermined (let N be large enough) and solve it through the Singular Value Decomposition approach (Press *et al.*, 1996).

Let us recall that $\mathbf{A}$ depends only on the departures of $\{\vec{\mathbf{e}}_j\}$-frame from orthogonality. Therefore we can choose the mapping matrix C (in expression $\mathbf{A} = \mathbf{C}\mathbf{C}^*$) as follows:

$$\mathbf{C} = \begin{matrix} 1 & 0 & 0 \\ -\sin\alpha & \cos\alpha & 0 \\ C_{31} & C_{32} & C_{33} \end{matrix}$$

with

$$\begin{aligned} C_{31} &= \frac{\tan\theta}{\sqrt{1 + \tan^2\theta + \tan^2\gamma}} \\ C_{32} &= \frac{\tan\gamma}{\sqrt{1 + \tan^2\theta + \tan^2\gamma}} \\ C_{33} &= \frac{1}{\sqrt{1 + \tan^2\theta + \tan^2\gamma}} \end{aligned}$$

which comes down to consider the orthonormal $\{\vec{\mathbf{u}}_j\}$-frame such that $\vec{\mathbf{e}}_1$ coincides with $\vec{\mathbf{u}}_1$, $\vec{\mathbf{e}}_2$ is in the $(\vec{\mathbf{u}}_1, \vec{\mathbf{u}}_2)$-plane and makes angle α with $\vec{\mathbf{u}}_2$, projections of $\vec{\mathbf{e}}_3$ onto the $(\vec{\mathbf{u}}_1, \vec{\mathbf{u}}_3)$ and $(\vec{\mathbf{u}}_2, \vec{\mathbf{u}}_3)$ planes make angles θ and γ with $\vec{\mathbf{u}}_3$. The absolute orientation of $\{\vec{\mathbf{u}}_j\}$ remains unknown as well as the $\{\vec{\mathbf{e}}_j\}$ ones. This $\vec{\mathbf{u}}_j$ frame can be called the orthonormal frame of the sensor.

Now we can explicitly express the entries of C and Λ from the entries of

$$\mathbf{G}^{-1} = \Lambda \mathbf{A} \Lambda^* = \Lambda \mathbf{C}\mathbf{C}^* \Lambda^*$$

and finally determine uniquely the values of α, θ, γ, β^1, β^2, β^3 (details in Appendix A). This closes the internal calibration process.

3.5 Remarks

Before presenting an application, we will make some general comments and warnings.

I) As clear from Eqs. (11) we need only the $\{\vec{\mathbf{H}}_k\}$ part of the initial data $\{b_k, \vec{\mathbf{H}}_k\}$ to determine the internal calibration parameters $\cos(\widehat{\vec{\mathbf{e}}_k \vec{\mathbf{e}}_j})$ and β^j. However, to recover the components of the $\vec{\mathbf{B}}_k$, we need the complete set of data.

II) Considering the linear system (11), it appears that the accuracy on the entries of the matrix $\mathbf{G}$ cannot be better than the accuracy on the $\{\vec{\mathbf{H}}_k\}$ part of the initial data. Taking into account that internal angles $\widehat{\vec{\mathbf{e}}_k \vec{\mathbf{e}}_j}$ and β^j are computed from these entries, we get an obvious limitation for the accuracy of the answer to the first part of the calibration problem.

III) Since $\mathbf{A}$ can be assumed not far from unit matrix, linear relation (8) shows that the significant digits in decimal representations of $\vec{\mathbf{B}}$ and $\vec{\mathfrak{B}} = (\mathcal{B}^1, \mathcal{B}^2, \mathcal{B}^3)$ are the same. In contrast, as already pointed out in Subsection 2.2, relations (5) and/or (6) show that magnitude orders of h^j and $\mathcal{B}^j$ are different due to the coefficients $b^{-1}\beta^j$. The number of significant digits in the answer for $\mathcal{B}^j$ cannot exceed the corresponding number of significant digits in the decimal representation of h^j. Therefore,

having b-value in pT—with eight significant digits and of the order of $5 \cdot 10^7$—, and assuming that we want also the values of $\vec{\mathbf{B}}$ in pT, we need the h-values with at least eight significant digits. With six digits in data precision and calculations the vectorial magnetic field measurements accuracy can be at best 0.1 nT.

According to this observation, the algorithm must be tested against several possible accuracy levels in data and the amount of data involved.

We tested the algorithm using synthetic data sets of 20 or 40 records $\left\{b_k, \vec{\mathbf{H}}_k\right\}$, assuming the precision of $\vec{\mathbf{H}}_k$ to be six significant digits. The resulting absolute errors for the recovered β^j and recovered mutual angles between the sensor axes appear to be independent of the values of the angles (the deformation). For 20 records the β^j errors are less than $1.0 \cdot 10^{-4}$ nT, the errors on mutual angles are less than $2.5 \cdot 10^{-6}\ rad$ (let us recall than the β^j are of the order of 50 nT). The corresponding error bounds for 40 records are approximately 1.5-times smaller, i.e. $7.0 \cdot 10^{-5}$ and $1.5 \cdot 10^{-6}$. Taking into account that there are only six significant digits in the decimal representation of h^j, we can conclude that 40 records are enough to provide the suitable precision for the internal calibration.

4. Processing Actual Data Delivered by the Magnetometer

When processing the data, we distinguish two types of errors that might occur in our measurements b_k, h_k^1, h_k^2, h_k^3:

I) Some measurements $\left\{b_k, h_k^1, h_k^2, h_k^3\right\}$ (for few exceptional k) appear to be completely out of range.

II) Some noise is present in each measurement; we may treat it as an additional random summand with a small mean and a variance of the order of, say, 1 nT.

When the calibration process uses a relatively small amount of data, the resulting uncertainties in the final answer due to these two different types of errors are not of the same order. Note indeed that a few bad lines in the sense of type I present in the data may cause large effects since the actual calibration algorithm uses a linear scheme. In the first tests of the magnetometer, a number of type I lines were affecting the measurements. It is no longer the case. Nevertheless we present in Appendix B the scheme (which could be of more general application) used to get rid of type I errors. This test is based on a simple statistical comparison of several independent calibrations.

In order to test the algorithm with respect to type II errors, a sequence of synthetic perfect measurements was prepared and then distorted by adding various levels of white noise. Tests on this simulated data showed that the algorithm is stable with respect to errors of type II, namely that the resulting uncertainty on the field components has the same order of magnitude as the noise level on the h measurements (in relative values). This looks natural since the calibration algorithm is based on two linear procedures: singular value decomposition and inversion of a matrix which is not far from the unit matrix.

5. Preliminary Experimental Results

In order to validate the calibration procedure on experimental data, it is necessary to record a statistically relevant dataset (i.e. a data set corresponding to a large and homogeneous enough distribution of directions of the $\vec{\mathbf{B}}$ vector with respect to the sensor axes to recover accurately the angles between these axes) Indeed, for a given orientation, the quantity of information contained in the corresponding line of data may be quite different for the different directions $\vec{\mathbf{e}}_i$. Two ways can be used to get such a dataset. We can artificially rotate the field around the sensor, or rotate the sensor itself in the geomagnetic field.

5.1 Rotating the magnetic field

Using an external coils system, it is possible to rotate the field seen by the sensing cell relatively to the modulation axes. As we just need to control approximately the field modulus and direction (we only use the measurements b_k, h_k^j of the helium sensor in this internal calibration process), such a device is easy to build. Starting from the knowledge of the mean value of the geomagnetic field, one cancels (still approximately) this field and adds the rotating one. The only constraint is that the direction of the resulting field has to cover a large range of directions. Moreover this technique allows to build automatic procedures where the generation of the rotating field and its measurement are simultaneous and continuous. Unfortunately, this method presents serious drawbacks in our case. An extra noise of 5 pT/$\sqrt{\text{Hz}}$ is indeed introduced by the external coils set (a stable current source is used; the field generated by the coils is of the same order as the geomagnetic field, a few tens of μT). This noise in the frequency domain of the modulations results in a 10^3 higher noise, i.e. 5 nT/$\sqrt{\text{Hz}}$, on the components measurement, due to the respective values of b and β, as explained in Subsection 2.1. This therefore deteriorates seriously the performances of the vector magnetometer and, consequently, the effectiveness of the corresponding calibration procedure.

5.2 Rotating the sensor

Data used in the following section have been obtained by rotating the sensor itself relatively to the geomagnetic field. The sensor output has been recorded with the magnetometer in a number of different orientations obtained by successive rotations: first rotations $R(\phi, \vec{\Omega}_1)$ around a vertical axis $\vec{\Omega}_1$ ($\phi = 0, 20, 40, \ldots 340^{\text{o}}$), then around a vector $\vec{\Omega}_2$ inclined by 20^{o} from the vertical, followed by a third set of rotations around $\vec{\Omega}_3$ coplanar with $(\vec{\Omega}_1, \vec{\Omega}_2)$ and 20^{o} from $\vec{\Omega}_2$, and so on till $\vec{\Omega}_9$, 10^{o} away from the vertical. We use then 180 orientations of the sensor, and make some 75 measurements in each of them. As a result, a data set of some 15000 data $\left\{b_k, \vec{\mathbf{H}}_k\right\}$ can be used for the calibration process which lasted approximately three hours.

A relevant and classical criterion to estimate the quality of the parameters reconstruction is the magnitude of the modulus residual, that is to say the difference between the measured modulus b and the reconstructed modulus B_{rec} using the vector measurements. A good estimate of the six parameters $(\beta^j, \widehat{(\vec{\mathbf{e}}^i, \vec{\mathbf{e}}^j)})$ is obtained when this difference is stable over the whole dataset, i.e. when no fluctuation of its mean value is observed while the magnetometer is rotated.

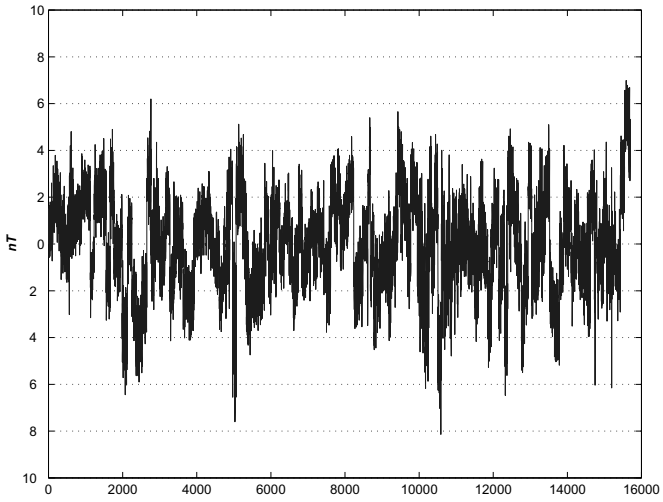

Fig. 5. Experimental modulus residual (difference between the reconstructed modulus and the measured one) obtained when rotating the sensor in the earth magnetic field. In abscissae, the number of the measurement.

In order to appreciate the results, we have first to examine the following question: suppose the algorithm has found the optimum solution, i.e. the right calibration parameters, what peak to peak residual will be seen on the modulus difference? If the peak to peak value of the noise v^i on the measurements B^i is small compared to the value of b, the residual $r = B_{\text{rec}} - b$ will be:

$$r = B_{\text{rec}} - b = \sqrt{\sum_{i=1}^{3} (B^i + v^i)^2} - b \sim \sum_{i=1}^{3} \frac{B^i}{b} v^i \quad (12)$$

(the noise on b is much smaller)

Considering v^i as three identical centered white noises (same variance σ_v^2), the variance of the residual may be written as the sum of the variances of the three distributions $v^i B^i / b$:

$$\sigma_r^2 = \sum_{i=1}^{3} \left(\frac{B^i}{b} \right)^2 \sigma_v^2. \quad (13)$$

Hence, the vector resolution being 1 nT/$\sqrt{\text{Hz}}$ with a 1 Hz bandwidth (as discussed in Subsection 2.2), the RMS noise on the scalar residual will be $\sigma_r \cong 1$ nT. The peak to peak noise is six times this value:

$$(B_{\text{rec}} - b)_{p-p} \cong 6 \text{ nT}. \quad (14)$$

Experimentally, the observed peak to peak value is close to 6 nT (see Fig. 5). Looking closer to Fig. 5, one can see indeed that locally the peak to peak value is of the order of the calculated limit. Thus the parameter set obtained is not far from the optimum. However, a low frequency fluctuation remains on the scalar residual which reflects small fluctuations in the vector measurements. A tentative explanation of such variations is that bandwidth fluctuations affect the scalar helium pumped magnetometer so that transfer functions seen by the three modulations vary slightly with time. Further possible improvements can be imagined. First of all, those bandwidth fluctuations could be reduced by working on the stability of the resonance excitation mechanism (laser or radio frequency oscillator). The bandwidth itself could be enlarged (working on the electronics frequency together with a new operating point in terms of RF amplitude and light power) in such a way that the influence of the fluctuations at the modulation frequencies would be reduced. But the most efficient way of getting rid of this low frequency noise is to correct its effect by modeling the scalar bandwidth and then forcing the scalar residual to zero in order to estimate the scalar cutoff frequency.

The accuracy of the so obtained β^i, α, θ, γ values has been also estimated by drawing randomly 200 subsets of 1000 data $\{b, h^1, h^2, h^3\}$ quadruplets from the 16000 ones available, and studying the dispersion of the corresponding 200 calibrations. Results are the following;

Departures from orthogonality are, in degrees:

$$\alpha = -0.1479^\circ, \quad \theta = 0.0015^\circ, \quad \gamma = 0.0026^\circ,$$

with an uncertainty of $4 \cdot 10^{-4}$ deg $= 7 \cdot 10^{-6}$ rad. Modulation values β are of the order of 50 000 pT with an accuracy of .2 pT (compare with the $1.5 \cdot 10^{-6}$rad and $7 \cdot 10^{-5}$ nT values of Subsection 3.5 for the case of synthetic data). These accuracies are close to the ones requested to obtain the B^i components with six significant digits.

6. Conclusion

In the introduction we presented the vector ^{4}He pumped magnetometer as a possible candidate for an automatic absolute magnetic observatory. Results obtained up to now and presented here lead us to think that the corresponding requested performances—see Introduction—should likely be obtained. Efforts are still to be made, mainly to reduce the long bandwidth fluctuations which affect the scalar helium magnetometer. Tests of a possible compensation of these fluctuations (the best solution to mitigate them as said above) are currently performed, with encouraging results.

Coming back to the calibration process, the method re-

tained here appears efficient. Let us stress again that we solve the problem using a linear algorithm. This algorithm can be extended to the calibration of satellite magnetometers as the Ørsted one (made of three fluxgate sensors and one scalar RMN) (Olsen *et al.*, 2000); apparently the linearity of the problem was not seen before. As already stressed, the data used in the calibration process allow an "internal" calibration: angles between the physical axes of the sensor are determined. Determining the exact orientation of these axes with respect to the geographical axes (OX-North, OY-East, OZ-downward vertical) should not be too difficult in a magnetic observatory where independent absolute measurements are available, but not trivial. Recall indeed that, contrarily to variometers operated in classical observatories, which measure only small relative variations of the field components, an absolute automatic magnetometer measures these full components, and consequently its axes must be known with a high accuracy. Of course, we have not addressed here the problem of the stability of pillars.

Now, providing a new version of ASMO is not our only objective. The ^{4}He vector magnetometer might also be advantageously used in space. Indeed, the resulting instrument has reasonable dimensions (size, weight and power consumption). Its main advantage is the replacement of the actual classical combination of a standard classical fluxgate vector magnetomer plus an absolute scalar magnetometer. The scalar and vector measurements are obtained continuously, simultaneously and at the same point, which might simplify the design of a satellite carrying this sensor, and the treatment of the resulting data. Thus, this vector helium pumped magnetometer seems very well suited for the needs of a satellite instrument.

Acknowledgments. First author was supported by CNES and CEA (Thèse CTCI). Second author was partly supported by grant INTAS/CNES 97-1048.

Appendix A. Recovering Λ and A

We consider the composition $\Lambda\mathbf{C}$ of the stretching matrix

$$\Lambda = \begin{matrix} \lambda_{11} & 0 & 0 \\ 0 & \lambda_{22} & 0 \\ 0 & 0 & \lambda_{33} \end{matrix}$$

(here $\lambda_{ii} = \beta^i > 0$) and the deformation matrix $\mathbf{C}$

$$\mathbf{C} = \begin{matrix} 1 & 0 & 0 \\ -\sin\alpha & \cos\alpha & 0 \\ C_{31} & C_{32} & C_{33} \end{matrix}$$

with

$$C_{31} = \frac{\tan\theta}{\sqrt{1+\tan^2\theta+\tan^2\gamma}}$$
$$C_{32} = \frac{\tan\gamma}{\sqrt{1+\tan^2\theta+\tan^2\gamma}}$$
$$C_{33} = \frac{1}{\sqrt{1+\tan^2\theta+\tan^2\gamma}}.$$

The last step of the internal calibration problem consists in recovering angles α, θ, γ and coefficients λ_{11}, λ_{22}, λ_{33} from the (already known – see Subsection 3.4) entries of the matrix $\mathbf{G}^{-1} = (\Lambda\mathbf{C}\mathbf{C}^*\Lambda^*)$. The entries of the 3×3 matrix $\mathbf{G}^{-1} = \mathbf{C}\mathbf{C}^*$ are:

$$\begin{matrix} \lambda_{11}^2 & -\lambda_{11}\lambda_{22}\sin\alpha & \left(\mathbf{G}^{-1}\right)_{13} \\ -\lambda_{11}\lambda_{22}\sin\alpha & \lambda_{22}^2 & \left(\mathbf{G}^{-1}\right)_{23} \\ \left(\mathbf{G}^{-1}\right)_{31} & \left(\mathbf{G}^{-1}\right)_{32} & \lambda_{33}^2 \end{matrix}$$

with

$$\left(\mathbf{G}^{-1}\right)_{13} = \frac{\lambda_{11}\lambda_{33}\tan\theta}{\sqrt{1+\tan^2\theta+\tan^2\gamma}}$$
$$\left(\mathbf{G}^{-1}\right)_{23} = \frac{\lambda_{22}\lambda_{33}\left(\cos\alpha\tan\gamma-\sin\alpha\tan\theta\right)}{\sqrt{1+\tan^2\theta+\tan^2\gamma}}$$
$$\left(\mathbf{G}^{-1}\right)_{31} = \frac{\lambda_{11}\lambda_{33}\tan\theta}{\sqrt{1+\tan^2\theta+\tan^2\gamma}}$$
$$\left(\mathbf{G}^{-1}\right)_{32} = \frac{\lambda_{22}\lambda_{33}\left(\cos\alpha\tan\gamma-\sin\alpha\tan\theta\right)}{\sqrt{1+\tan^2\theta+\tan^2\gamma}}.$$

So, after computing the entries of the matrix $\mathbf{G}^{-1}$, we straightforwardly get unique (positive) values of λ_{11}, λ_{22}, λ_{33} and $\sin\alpha$. Taking into account that $\alpha < \frac{\pi}{2}$ we find $\cos\alpha$ and then (after substitution and simplification) get the following elementary system of equations:

$$\begin{cases} \dfrac{\tan\theta}{\sqrt{1+\tan^2\theta+\tan^2\gamma}} = p \\ \dfrac{\tan\gamma}{\sqrt{1+\tan^2\theta+\tan^2\gamma}} = q \end{cases}$$

where q and p are known values since λ_{11}, λ_{22}, λ_{33} and α are known. It has the explicit solution

$$\begin{cases} \tan^2\theta = \dfrac{p^2}{1-p^2-q^2} \\ \tan^2\gamma = \dfrac{q^2}{1-p^2-q^2} \end{cases}.$$

For $\theta, \gamma < \frac{\pi}{2}$ this provides an unique solution. The simple numerical algorithm for calibration is clear from above.

Appendix B. Case of a Few Bad Lines in the Data

The dataset is made of N vectors $(b_k, h_k^1, h_k^2, h_k^3)$, and we may assume that $m \ll N$ indices k out of N correspond to error measurements. First recall that $N \sim 50$ typically is enough to provide a reasonable precision answer (see Remarks 3.5). If $N \gg 10^2$ we can make several calibrations based on random subsets of indexes $\{k_1, \dots k_n\} \subset \{1, \dots N\}$, $n \sim 10^2$. The probability p that the random subset $\{k_1, \dots k_n\}$ does not include any "bad" index is

$$p = p(n,m,N) = \frac{\binom{N-m}{n}}{\binom{N}{n}}$$
$$= \frac{(N-m)(N-m-1)\dots(N-m-n+1)}{N(N-1)\dots(N-n+1)}$$
$$= \left(1-\frac{m}{N}\right)\left(1-\frac{m}{N-1}\right)\dots\left(1-\frac{m}{N-n+1}\right).$$

Then $0 < p < 1$ for $n + m \leqslant N$. Fix n and consider $l < \binom{N}{n}$ calibrations corresponding to random subsets $\{k_1, \ldots k_n\} \subset \{1, \ldots N\}$. Then (from the binomial distribution) the probability P that there are at least two *proper* (i.e. free of error data) calibrations is given by

$$P = P(l, p) = 1 - (1 - p)^l - l \cdot p(1 - p)^{l-1}.$$

If $m \ll N$ is small and N large enough, one can easily find the corresponding values for n and l ensuring a probability P statistically significant. Then in a statistical sense we will have at least two proper (and therefore close to each other, up to a given precision) calibrations. Taking into account that *non-proper* (i.e. based on data including bad lines) calibrations will present strong deviations from each other and from the true calibration, we have only to find two close enough answers out of l.

References

Alldredge, L. R., A proposed automatic standard magnetic observatory, *J. Geophys. Res.*, **65**, N11, 3777–3786, 1960.

Alldredge, L. R. and I. Saldukas, An automatic standard magnetic observatory, *J. Geophys. Res.*, **69**, N10, 1963–1970, 1964.

Colegrove, F. D. and L. D. Schearer, Optical pumping of helium in the $^3S_1$ metastable state *Physical Review*, **119**, 680–690, 1961.

Guttin, C., J.-M. Léger, and F. Stoeckel, Realization of an isotropic scalar magnetometer using optically pumped helium 4, *Journal de Physique III*, **4**, 655–659, 1993.

Merayo, M. G., P. Brauer, F. Primdhal, J. R. Petersen, and O. V. Nielsen, Scalar calibation of vector magnetometer, *Meas. Sci. Technol.*, **11**, 120–132, 2000.

Nielsen, O. V., J. R. Petersen, F. Primdhal, P. Brauer, B. Hernando, A. Fernández, M. G. Merayo, and P. Ripka, Development, construction and analysis of the Orsted fluxgate magnetometer, *Meas. Sci. Technol.*, **6**, 1099–1115, 1995.

Olsen, N., L. Toffner-Clauden, T. Risbo, P. Brauer, J. Merayo, F. Primdhal, and T. Sabaka, In-Flight calibration methods used for the Oersted mission, in *ESA SP on Space Magnetometer Calibration*, 2000.

Press, C., S. Teukolsky, W. Vetterling, and B. Flannery, *Numerical Recipes in C. Second edition*, Cambridge University Press, Cambridge, 1996.

Rasson, J. L., Proceedings of the VIth Workshop on Geomagnetic Observatory Instruments Data Acquisition and Processing, publication scientifique et technique n 003, Institut Royal Météorologique de Belgique, Avenue Circulaire 3, B-1180 Bruxelles.

Trigg, D. F. and R. L. Coles, Intermagnet, technical reference manual, 1999.

O. Gravrand, A. Khokhlov (e-mail: khokhlov@mitp.ru), J. L. Le Mouël, and J. M. Léger